

A development of lifetime measurement based on the differential decay curve method

Jian Zhong¹ · Xiao-Guang Wu¹ · Ying-Jun Ma² · Yun Zheng¹ · Cong-Bo Li¹ ·
Guang-Sheng Li¹ · Bao-Ji Zhu¹ · Tian-Xiao Li^{1,3} · Yan-Jun Jin¹ · Yan-Xiang Gao¹ ·
Ke-Yan Ma² · Dong Yang² · Hao Guo² · Jia-Qi Wang² · Xian Guan² ·
Ji Sun²

Received: 22 March 2018 / Revised: 10 April 2018 / Accepted: 16 April 2018 / Published online: 3 July 2018
© Shanghai Institute of Applied Physics, Chinese Academy of Sciences, Chinese Nuclear Society, Science Press China and Springer Nature Singapore Pte Ltd. 2018

Abstract A new development of indirect gating case in the differential decay curve method used for lifetime measurement has been introduced. The gate region was extended from partial shifted peak to both shifted and unshifted components. The statistics of flight and stop peaks in gating spectra was improved obviously. The reliability of this change has been tested by reanalysing the lifetime of 2^+ state in ^{134}Ce . The result of 32.2(33) ps was fit well with the previous published values within the experimental uncertainty. The developed method was also used to analyse the lifetime of 2^+ state in ^{138}Nd .

Keywords Lifetime · The differential decay curve method · Gating region

This work was supported by the National Natural Science Foundation of China (No. 11475072, 11375267, 11305269, 11405274, 11405072, 11205069, 11775307, 11375266, 11575118 and 11605114), the National Natural Science Foundation of Guangdong, China (No. 2016A030310042), and the National Key Research and Development Program of China, the National Key Scientific Instrument and Equipment Development Projects, China (No. 2017YFF0106501).

✉ Jian Zhong
zhongj2015@163.com

Xiao-Guang Wu
wxg@ciae.ac.cn

Ying-Jun Ma
myj@jlu.edu.cn

¹ China Institute of Atomic Energy, Beijing 102413, China

² College of Physics, Jilin University, Changchun 621010, China

³ Shenyang Institute of Engineering, Shenyang 110136, China

1 Introduction

Transition probabilities are of special interest for the understanding of nuclear structure because of their sensitivity to the details of nuclear wave functions. Therefore, absolute transition probabilities or lifetime measurements of excited nuclear states are very important in γ -spectroscopy. Radiative lifetimes of excited nuclear levels in the picosecond region can be measured with the recoil distance Doppler shift (RDDS) method. The differential decay curve method (DDCM) [1–5], which has been proved to be a reliable analysis technique used for lifetime measurement data obtained from the RDDS experiments, such that mean lifetimes of excited states in nuclei can be determined precisely. For standard DDCM analysis in γ – γ coincident mode, the mean lifetime of interest level can be determined at every target-to-stopper distance by gating on the Doppler-shifted component of higher-lying transition. Thereafter, the normalized intensities of the stopped and Doppler-shifted γ rays for a transition depopulating this excited state were fitted with second-order polynomials, as described in Ref. [3], where one obtains two curves for the Doppler-shifted and unshifted components, which are used to extract the lifetime at each target-to-stopper distance. These curves are called coincidence decay curves.

The most significant errors associated with the measured mean-lifetime arise from the statistical uncertainties associated with the fitting of the decay curves and the range in the recoil velocities of the recoiling nuclei. In most of the work, there was a significant spread in recoil velocities due to the relatively low initial recoil velocity within the target. The low velocity of the recoiling compound nucleus results in a small energy separation between the stopped and Doppler-shifted peaks, which means that the shifted and

unshifted peaks in the coincident spectra will overlap each other (see Fig. 1). In order to ensure that the gating region set on a flight peak does not include any contaminant γ rays from the tail of the corresponding stop peak, only partial selection of the shifted component could be used as the feeding component (see gate 1 in Fig. 1). Two major disadvantages will be caused by gating on the partial shifted peak. Firstly, the mean recoil velocity should be modified in the data analysis because only high-speed flight nuclei in shifted components are selected for gating so it will bring some systematic deviations in the result. Secondly, the statistics of flight and stop peaks obtained from the gating partial shifted component in the spectra is usually poor and it is hard to fit the shifted and unshifted peaks.

In this paper, the Doppler-shifted and unshifted peaks instead of the partial shifted component were selected as the gating region (see gate 2 in Fig. 1). This change will be beneficial in avoiding the disadvantages mentioned above. The mean lifetimes of 2_1^+ states in ^{134}Ce and ^{138}Nd determined by the new gating region were performed to confirm the reliability of this method.

2 Experimental details

The present work was performed at the HI-13 tandem accelerator of the China Institute of Atomic Energy (CIAE) in Beijing. Excited states in ^{138}Nd were populated using the $^{123}\text{Sb}(^{19}\text{F}, 4n)^{138}\text{Nd}$ fusion–evaporation reaction at a beam energy of 87 MeV. A 0.62 mg/cm^2 thick ^{123}Sb foil, which was evaporated on a 2.2 mg/cm^2 thick Ta backing facing the beam, was used as the target. The flying residues nuclei were stopped by a 10 mg/cm^2 thick Ta stopper. The mean recoil velocity of the compound nucleus was $\sim 1\%$ of the

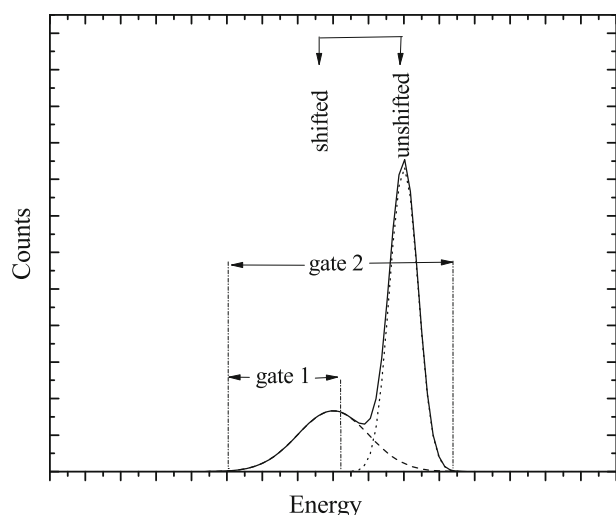


Fig. 1 Sample for the gated region in the DDCM

light speed, c . The lifetime measurement was taken by the RDDS method using the CIAE plunger device, which has been introduced in Ref. [6] and was utilized to set and keep the distance between the target and stopper with a relative precision of $0.3\ \mu\text{m}$. Eight Compton-suppressed high-purity Ge (HPGe) detectors were utilized to detect the deexcited γ -rays from the reaction residues. Three of these detectors were placed at 90° , four at 153° , and one at 42° with respect to the beam direction. The detectors were calibrated for γ -ray energies and efficiencies using the ^{133}Ba and ^{152}Eu standard sources. Thirteen different target-to-stopper distances, 5, 9, 15, 25, 41, 70, 100, 166, 275, 457, 758, 1259, and $2000\ \mu\text{m}$ were used to record the γ - γ coincidences data. For the data analysis of the lifetime of 2_1^+ state in ^{138}Nd , only distance points shorter than $457\ \mu\text{m}$ were used.

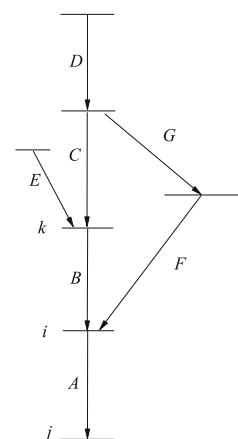
3 Data analysis method

To simplify the calculation, the following discussion just contains the simple situation of γ - γ coincidence analysis in the DDCM. More complex detail can be found in Ref. [3, 5]. According to the DDCM, the mean lifetime, τ , of the level i that is depopulated via transition A can be determined at every plunger distance x by gating either “indirectly” or “directly” (see Fig. 2). In the indirectly gating case, a gate is set on the Doppler-shifted component of a transition, say C , that depopulates a higher-lying state and feeds the level i , via intermediate transitions the last of which is the transition B , which directly feeds level i . Then, the time evolution of the population, $n_i(t)$, of the state i is given by the well-known differential equation:

$$\frac{d}{dt}n_i^{CA}(t) = -\lambda_i n_i^{CA}(t) + \lambda_k n_k^{CB}(t), \quad (1)$$

where $n_i^{CA}(t)$ is the number of nuclei in the state i at the time, t , which is populated and decays via the cascade

Fig. 2 Level scheme sample for direct and indirect gating



$C \rightarrow B \rightarrow A$. And λ_i denotes the decay constant of level i . Then, the lifetime, τ_i , can be expressed as:

$$\tau_i(t) = \frac{-N_i^{CA}(t) + N_k^{CA}(t)}{\frac{d}{dt}N_i^{CA}(t)} \tag{2}$$

Here $N_A^{CA}(t) = N_i^{CA}(t) = \lambda_i \int_t^\infty n_i^{CA}(t)dt$ and $N_B^{CA}(t) = N_k^{CA}(t) = \lambda_k \int_t^\infty n_k^{CA}(t)dt$, because only the coincident cascade $C \rightarrow B \rightarrow A$ in Fig. 2 was considered in the present discussion.

As can be seen in the discussion above, the time information of the coincident intensity must be contained in the lifetime measurement. To simplify the discussion, it is useful to define the notation $I_{(s,u)}^{CA}$ as the coincident intensities of the unshifted (u) peak of transition A which is gated by the shifted (s) peak of transition C . If time, t , is the flight time of the recoil nuclei between creation in the target and arriving at the stopper, which means that the range of integration in Eq. (2) donates the intensities of unshifted component in gating spectra, then can be identified N_i^{CA} with $I_{(u+s,u)}^{CA}$, and $N_k^{CA}(t)$ with $I_{(u+s,u)}^{CB}$. Eq. (2) can be rewritten as:

$$\tau_i(t) = \frac{-I_{(u+s,u)}^{CA}(t) + I_{(u+s,u)}^{CB}(t)}{\frac{d}{dt}I_{(u+s,u)}^{CA}(t)} \tag{3}$$

According to the time interval in the DDCM analysis, the coincident intensities in gating spectra can be split into several parts as follow:

$$\begin{aligned} I_{(u+s,u+s)}^{CA} &= I_{(u+s,s)}^{CA} + I_{(u+s,u)}^{CA} \\ &= I_{(u,s)}^{CA} + I_{(s,s)}^{CA} + I_{(u,u)}^{CA} + I_{(s,u)}^{CA} \end{aligned} \tag{4}$$

Obviously, $I_{(u,s)}^{CA}$ is equal to zero for the time order of transitions. Because $I_{(u+s,u+s)}^{CA}$ is independent of time, t , a useful relation can be derived from Eq. (4) as:

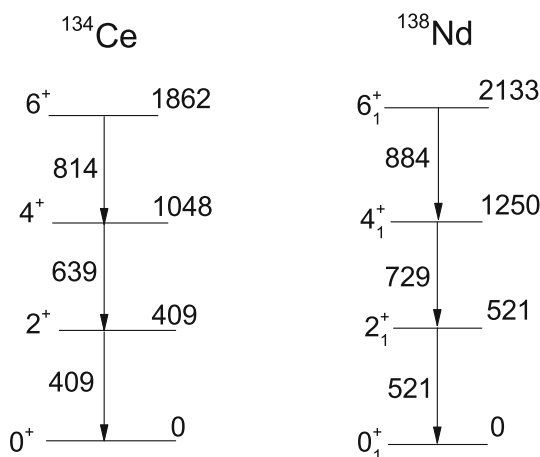


Fig. 3 Partial level scheme of ^{134}Ce and ^{138}Nd . Information is taken from ^{134}Ce [9], ^{138}Nd [10]

$$\frac{d}{dt}I_{(u+s,u)}^{CA}(t) = -\frac{d}{dt}I_{(u+s,s)}^{CA}(t) = -\frac{d}{dt}I_{(s,s)}^{CA}(t) \tag{5}$$

Then, Eq. (3) can be rewritten as:

$$\tau_i(t) = \frac{I_{(u+s,u)}^{CA}(t) - I_{(u+s,u)}^{CB}(t)}{\frac{d}{dt}I_{(u+s,s)}^{CA}(t)} \tag{6}$$

or

$$\tau_i(t) = \frac{I_{(u+s,u)}^{CA}(t) - I_{(u+s,u)}^{CB}(t)}{\frac{d}{dt}I_{(s,s)}^{CA}(t)} \tag{7}$$

The coincidence intensities discussed above denote absolute values which are usually not observed in an experiment. The measured coincidence intensities are proportional to absolute values, and the factors depend on the efficiencies for detecting the transition and the angular correlations of these transitions, respectively. Evidently, the factors between obtained intensities and absolute values are not the same for different transitions in coincident gating spectra, and the modifying factor for this difference is defined as α . In order to compare coincidence intensities, the following ratio is valid:

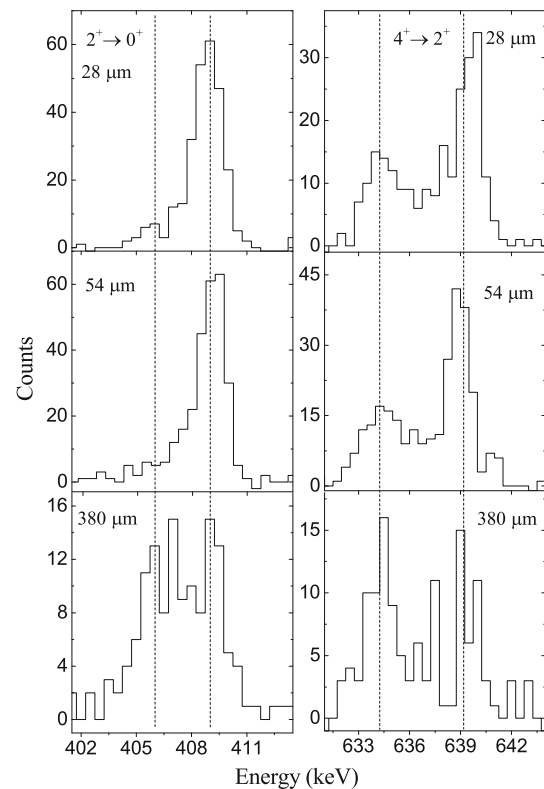


Fig. 4 Left: Projected stopped and backward-shifted components for the 409 keV, $2^+ \rightarrow 0^+$ transition in ^{134}Ce from gating on the backward-shifted and unshifted components of the 814 keV transition. Right: Corresponding backward-shifted and unshifted components of the 639 keV $4^+ \rightarrow 2^+$ transition

$$\alpha = \frac{I_{(u+s,u+s)}^{CA}}{I_{(u+s,u+s)}^{CB}} = \frac{I_{(s,u+s)}^{CA}}{I_{(s,u+s)}^{CB}} = \frac{I_{(u,u+s)}^{CA}}{I_{(u,u+s)}^{CB}} = \frac{I_{(u,u)}^{CA}}{I_{(u,u)}^{CB}}. \tag{8}$$

Using the observed coincidence intensity quantities, one gets:

$$\tau_i(t) = \frac{I_{(u+s,u)}^{CA}(t) - \alpha \cdot I_{(u+s,u)}^{CB}(t)}{\frac{d}{dt} I_{(u+s,s)}^{CA}(t)} \tag{9}$$

or

$$\tau_i(t) = \frac{I_{(u+s,u)}^{CA}(t) - \alpha \cdot I_{(u+s,u)}^{CB}(t)}{\frac{d}{dt} I_{(s,s)}^{CA}(t)}. \tag{10}$$

Using Eq. (8), the numerator of Eq. (10) can be changed to:

$$\begin{aligned} & I_{(u+s,u)}^{CA} - \alpha \cdot I_{(u+s,u)}^{CB} \\ &= (I_{(s,u)}^{CA} + I_{(u,u)}^{CA}) - \alpha \cdot (I_{(s,u)}^{CB} + I_{(u,u)}^{CB}) \\ &= (I_{(s,u)}^{CA} - \alpha \cdot I_{(s,u)}^{CB}) + (I_{(u,u)}^{CA} - \alpha \cdot I_{(u,u)}^{CB}) \\ &= I_{(s,u)}^{CA} - \alpha \cdot I_{(s,u)}^{CB}. \end{aligned} \tag{11}$$

If v is the mean recoil velocity of the nuclei, then Eqs. (9) and (10) can be rewritten as:

$$\begin{cases} \tau_i(x) = \frac{I_{(u+s,u)}^{CA}(x) - \alpha \cdot I_{(u+s,u)}^{CB}(x)}{v \cdot \frac{d}{dx} I_{(u+s,s)}^{CA}(x)} \\ \alpha = \frac{I_{(u+s,u+s)}^{CA}(x)}{I_{(u+s,u+s)}^{CB}(x)} \end{cases} \tag{12}$$

or

$$\begin{cases} \tau_i(x) = \frac{I_{(s,u)}^{CA}(x) - \alpha \cdot I_{(s,u)}^{CB}(x)}{v \cdot \frac{d}{dx} I_{(s,s)}^{CA}(x)} \\ \alpha = \frac{I_{(s,u+s)}^{CA}(x)}{I_{(s,u+s)}^{CB}(x)}. \end{cases} \tag{13}$$

Moreover, a gate is often set on a direct feeding transition of the level of interest, e.g. a gate placed on the transition B is shown in Fig. 2. This means that only the coincidence cascade $B \rightarrow A$ was considered. The level of interest is fed only via transition B , and all other feeders are excluded, which means that the integral of $N_k^{CA}(t)$ in the numerator of Eq. (2) is changed into $N_B^{BA}(t) = N_k^{BA}(t) = \lambda_k \int_t^\infty n_k^{BA}(t) dt = I_{(u,u+s)}^{BA}(t)$. The numerator of Eq. (7) is changed to:

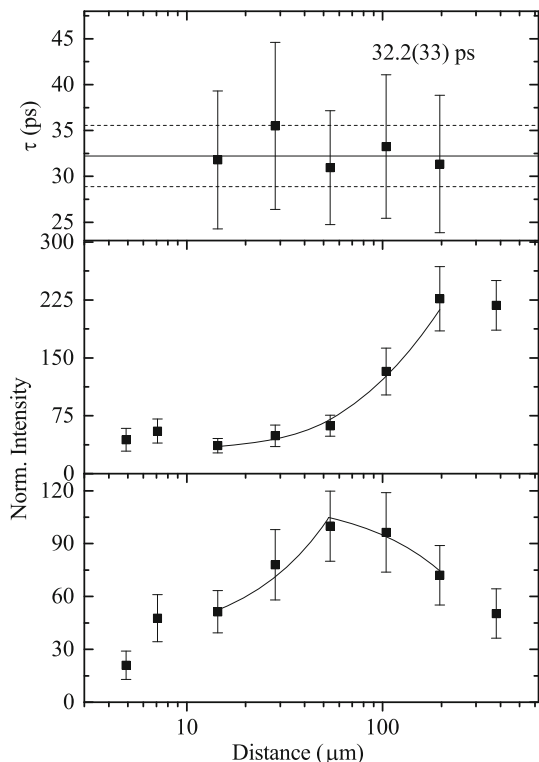


Fig. 5 Decay curves and lifetime determination of the 409 keV, $2^+ \rightarrow 0^+$ transition in ^{134}Ce . The middle and lower panel shows the Doppler-shifted and stopped intensities vs distance. The mean lifetime at each distance is determined (using Eq. (12)) and is shown in the upper panel as function of distance. The weighted average of these values yields the overall mean lifetime

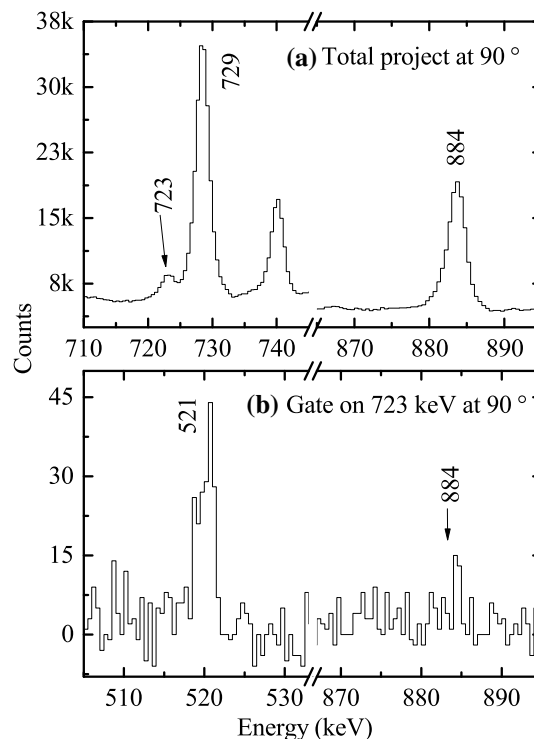


Fig. 6 **a** Total project of 90° in the lifetime measurement experiment of ^{138}Nd . The 723 keV γ -ray is a contaminate from ^{135}Ce ; **b** Background-corrected coincidence spectrum obtained by gating the 723 keV γ -ray at 90° , the 521 keV γ -ray peak can be seen in the gating spectrum clearly

$$\begin{aligned}
 I_{(u+s,u)}^{BA} - I_{(u,u+s)}^{BA} &= (I_{(s,u)}^{BA} + I_{(u,u)}^{BA}) - (I_{(u,u)}^{BA} - I_{(u,s)}^{BA}) \\
 &= I_{(s,u)}^{BA}.
 \end{aligned}
 \tag{14}$$

So for the direct gating case, the lifetime, τ_i :

$$\tau_i(x) = \frac{I_{(s,u)}^{BA}(x)}{v \cdot \frac{d}{dx} I_{(s,s)}^{CA}(x)}.
 \tag{15}$$

But in the present work, more attention was focused on the difference between Eqs. (12) and (13). As can be seen from the discussion above, these two equations were both derived from the time differential equation (Eq. (1)). The difference occurred in Eq. (5). Denominators of Eqs. (12) and (13) are the second term and third term of Eq. (5), respectively. However, for indirect gating case, only Eq. (13) is posed in Ref. [3], and then this equation was used widely in the latter indirect gating research. The main difference between these two equations is the gating region. In Eq. (12), coincident intensities were deduced by setting a cut on both Doppler-shifted and unshifted ($u + s$) components of a higher-lying transition. But in Eq. (13), only a partial shifted (s) peak was selected as the gating region.

4 Results

Two experimental data have been analysed to confirm that the new gating region selection can help to improve the statistics of flight and stop peaks in the gating spectra. The first comparison is that the lifetime measurement of 2^+ state in ^{134}Ce , which has been presented in Ref. [7], was reanalysed with the new gating region, and the result reproduced the lifetime well within the experimental error.

The lifetime measurement of 2^+ state in ^{134}Ce was taken by Husar et al. as 32.7(28) ps in 1976 [8]. Then in 2016, this lifetime was remeasured by Zhu et al. as 33.8(28) ps [7]. Differentiated from the direct gating case used in Ref. [7], in this paper, the experimental data presented by Zhu et al. were reanalysed with an indirect gate setting on both the Doppler-shifted and unshifted components of the $6^+ \rightarrow 4^+$ 814 keV γ -ray transition (see Fig. 3). Partial gating spectra of the $4^+ \rightarrow 2^+$ 639 keV and the $2^+ \rightarrow 0^+$ 409 keV transitions are posed in Fig. 4. Shifted and unshifted normalized intensities of these two transitions were fit by the NAPATAU program [11]. And the result 32.2(33) ps derived from Eq. (12) was consistent with the previous results in Ref. [8] as well as Ref. [7] within the

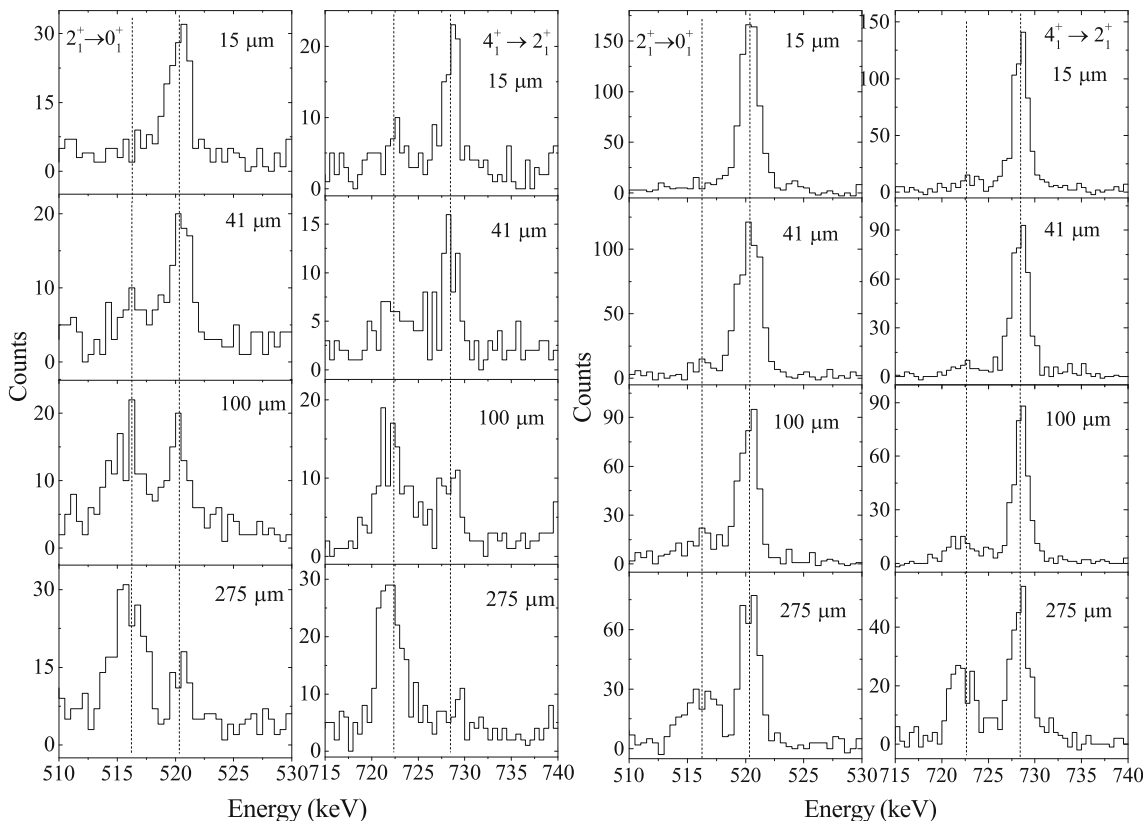


Fig. 7 Left: Projected stopped and backward-shifted components for the 521 keV, $2^+ \rightarrow 0^+$ transition and the 729 keV, $4^+ \rightarrow 2^+$ transition in ^{138}Nd from gating on the backward-shifted components

of the 884 keV $6^+ \rightarrow 4^+$ transition. Right: the same as left, but from gating on the backward-shifted and unshifted components of the 884 keV transition

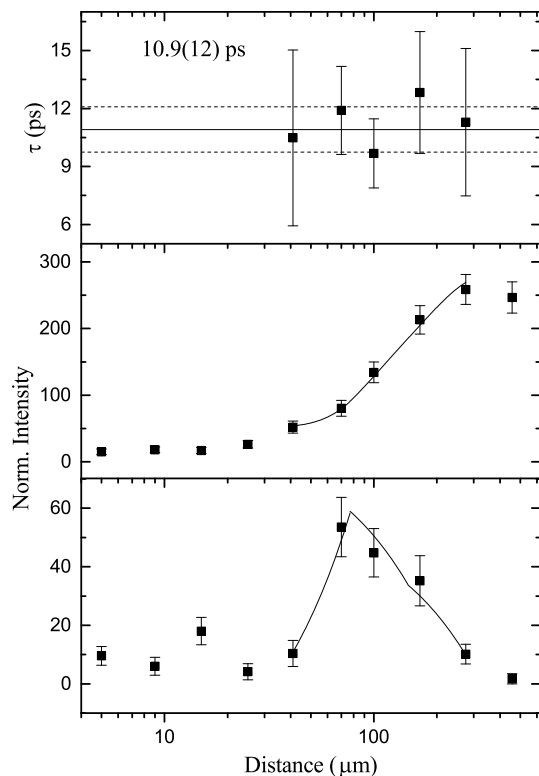


Fig. 8 The same as Fig. 5, but for the 521 keV, $2_1^+ \rightarrow 0_1^+$ transition in ^{138}Nd

experimental uncertainty, which means that Eq. (12) can also be used in the indirect gating case. The errors, $\Delta\tau$, of the present results were calculated as $\Delta\tau = \sqrt{\Delta\tau_{\text{st}}^2 + \Delta\tau_1^2 + \Delta\tau_2^2}$ where $\Delta\tau_{\text{st}}$ are the statistical errors. The systematic errors, $\Delta\tau_1$, are estimated uncertainties arising from contaminating lines that might be present but could not be observed directly in the present measurement. These values were estimated on the basis of a careful inspection of the total τ curves. Outside the sensitive range, the effects of contaminating lines show up in a pronounced way. In addition, it was taken into account how many different gates and different detectors were used in the data analysis because this is strongly correlated with the possibility of unobserved contaminations. The error $\Delta\tau_2 = 2\% \cdot \tau$ gives an estimate of systematic errors arising from several small effects for which no corrections were performed (Fig. 5).

The second comparison is peak shapes in gating spectra of the $2_1^+ \rightarrow 0_1^+$ transition in ^{138}Nd . Due to the neutron damage and poor statistics of forward (42°) detectors, only backward (153°) detectors were used to analyse the lifetime of the 2_1^+ state in ^{138}Nd . However, a 723 keV contaminate γ -ray was found in the left side of 729 keV $4_1^+ \rightarrow 2_1^+$ transition in the 90° spectrum (see Fig. 6). So the indirect gating case is suitable for the data

analysis of the lifetime of the 2_1^+ state in ^{138}Nd . In the present work, both gating regions described in Eqs. (12) and (13) were tried. As shown in Fig. 7, the wider the gating region selected, the better peak shapes of the Doppler-shifted and unshifted component can be taken in the gating spectra, especially for the spectra of long target-stopper distance. Finally, Eq. (12) is used to fit curves of the shifted and unshifted normalized intensities by the NAPATAU program [11], too. And the resultant coincidence decay curves and τ plot are shown in Fig. 8. From the resulting decay curves, the deduced mean lifetime of the 2_1^+ state in ^{138}Nd is 10.9(12) ps. The result will be used to identify the shape coexistence and evolution in ^{138}Nd in the future.

5 Summary

A new development of indirect gating case in the differential decay curve method has been introduced in the present work. The gate region was extended from partial shifted peak to both shifted and unshifted components. This change has been confirmed by reanalysing the lifetime of the 2^+ state in ^{134}Ce in Ref. [7]. The result of 32.2(33) ps was fit well with the previous published values [7, 8] within the experimental uncertainty. This development was also used to analyse the lifetime of 2_1^+ state in ^{138}Nd . The statistics of flight and stop peaks in the gating spectra was improved obviously. The lifetime 10.9(12) ps will be used in the further discussion.

References

1. T.K. Alexander, J.S. Forster, Lifetime measurements of excited nuclear levels by Doppler-shift methods. *Adv. Nucl. Phys.* **10**, 197–331 (1978). <https://doi.org/10.1007/978-1-4757-4401-9>
2. A. Dewald, S. Harissopoulos, P. von Brentano, The differential plunger and the differential decay curve method for the analysis of recoil distance Doppler-shift data. *Z. Phys. A* **334**, 163 (1989). <https://doi.org/10.1007/BF01294217>
3. G. Bohm, A. Dewald, P. Petkov et al., The differential decay curve method for the analysis of Doppler shift timing experiments. *Nucl. Instrum. Methods Phys. Res. A* **329**, 248–261 (1993). [https://doi.org/10.1016/0168-9002\(93\)90944-D](https://doi.org/10.1016/0168-9002(93)90944-D)
4. P. Petkov, Errors arising from nuclear hyperfine interactions on lifetimes determined by the recoil distance Doppler shift method. *Nucl. Phys. A* **349**, 289–291 (1994). [https://doi.org/10.1016/0168-9002\(94\)90636-X](https://doi.org/10.1016/0168-9002(94)90636-X)
5. A. Dewald, O. Moller, P. Petkov, Developing the Recoil Distance Doppler-Shift technique towards a versatile tool for lifetime measurements of excited nuclear states. *Prog. Part. Nucl. Phys.* **67**, 786–839 (2012). <https://doi.org/10.1016/j.ppnp.2012.03.003>
6. Q.M. Chen, X.G. Wu, Y.S. Chen et al., Lifetime measurements in ^{180}Pt . *Phys. Rev. C* **93**, 044310 (2016). <https://doi.org/10.1103/PhysRevC.93.044310>

7. B.J. Zhu, C.B. Li, X.G. Wu et al., Investigation on anomalously low $B(E2; 4_1^+ \rightarrow 2_1^+)/B(E2; 2_1^+ \rightarrow 0_1^+)$ ratio in ^{134}Ce through lifetime measurements. *Phys. Rev. C* **95**, 014308 (2017). <https://doi.org/10.1103/PhysRevC.95.014308>
8. D. Husar, J.S. Mills, H. Craf et al., Observed Retardation of the $E2$ Transitions in the Backbending Region of ^{134}Ce . *Phys. Rev. Lett.* **36**, 1291 (1976). <https://doi.org/10.1103/PhysRevLett.36.1291>
9. C.M. Petrache, S. Guo, A.D. Ayangeakaa et al., Triaxiality and exotic rotations at high spins in ^{134}Ce . *Phys. Rev. C* **93**, 064305 (2016). <https://doi.org/10.1103/PhysRevC.93.064305>
10. C.M. Petrache, S. Frauendorf, M. Matsuzaki et al., Tilted axis rotation, candidates for chiral bands, and wobbling motion in ^{138}Nd . *Phys. Rev. C* **86**, 044321 (2012). <https://doi.org/10.1103/PhysRevC.86.044321>
11. B. Saha, computer code NAPATAU, unpublished (Institute of Nuclear Physics, Cologne)